Relative Seismic Risk Evaluation of Various Buildings Based on an Input Wave Field

Masahiro Iida, A.M.ASCE[1]; Masanori Iiba[2]; Koichi Kusunoki[3]; Yuji Miyamoto[4]; and Hiroshi Isoda[5]

Abstract: Seismic responses of various buildings are calculated by a three-dimensional (3D) linear method for examining the soil-building interaction based on an input seismic wave field in the reclaimed zone of Tokyo Bay in which ground motions include a considerable amount of surface waves. A seismic wave field means seismic waves propagate in a 3D medium. The method was recently proposed to adequately treat surface waves trapped by a deep (several kilometers) underground structure in a soil-building interaction system. First, seismic responses of a building were calculated at two soft-soil sites for three large earthquakes to understand the variations in building responses with reference to sites and earthquakes. Second, seismic responses of low- to high-rise reinforced concrete (RC) and steel buildings and wood buildings were compared at a soft-soil site for a large earthquake, evaluating the relative seismic risk of various buildings. Midrise RC and steel buildings shook more severely than low-rise and high-rise RC and steel buildings. Flexible wood buildings suffered extremely large interstory drifts, indicating the largest seismic risk. **DOI: 10.1061/(ASCE)GM.1943-5622.0000967.**

Introduction

Seismic dynamic behavior of reinforced concrete (RC), steel, and wood buildings has been investigated intensively in numerous studies, using a variety of analytical, computational, and experimental techniques. Undoubtedly, the investigations have played a very important role in the understanding of building performance. In contrast, the investigations seem to concentrate on the superstructures of the buildings considerably. Soil-building interaction analysis has only a short history. The analysis was initiated in the 1950s (Housner 1957) and became popular starting in the 1970s (Flores-Berrones and Whitman 1982; Bielak and Christiano 1984). Relevant factors, such as building foundations, soils, and ground motions, are significant as well.

A soil-building interaction analysis is of great benefit when estimating the seismic response of a building with piles. In an interaction analysis, a building shakes not only with the natural periods of the building but also with the predominant periods of the ground. Theoretically, the vibration modes of a building are composed of building modes and soil modes. An interaction analysis is able to consider both modes properly. Also, in a soil-building interaction system, S-wave incidence and surface-wave incidence are used. However, although S-wave incidence into the interaction system is valid for estimating reasonable building responses, surface-wave incidence is not valid because short-period (less than a few seconds) seismic surface waves are trapped by a deep (several kilometers) underground structure.

The invalidity of the surface-wave incidence is caused by the inherent feature of surface waves that the vertical increase in the amplitudes of short-period surface waves in a shallow (several tens of meters) underground structure depends strongly on the material properties of the deep underground structure in which surface waves propagate. In other words, a sufficiently large model volume representing an appropriate deep structure is required for surface-wave incidence. This problem of surface waves was explained mathematically in a soil response study (Iida 2006).

To adequately treat short-period surface waves trapped by a deep underground structure in a soil-building interaction system, a three-dimensional (3D) linear FEM for examining the soil-building interaction based on an input seismic wave field was proposed (Iida 2013). An input seismic wave field means that forces produced by body and surface waves propagating in the 3D soil volume of the system are used as external forces in the finite-element (FE) calculations. This new treatment of seismic external force was successfully used for the first time in the soil response study (Iida 2006). Using the proposed method, seismic responses of low- to high-rise RC model buildings were successfully calculated during a large earthquake in the lake bed zone of Mexico City in which surface waves are dominant. The calculated building responses were consistent with the real damage pattern.

In a subsequent study (Iida et al. 2015), to reconfirm the validity of the proposed method, after a few improvements in the method were made, seismic building responses were estimated in the reclaimed zone of Tokyo Bay in which surface waves are dominant. The method successfully reproduced surface, downhole, and building accelerograms that were recorded at a borehole station during two medium-sized earthquakes. Also, seismic responses of a midrise RC building and a wood building were calculated at another borehole station for the 1923 Kanto earthquake (earthquake magnitude $M_J = 8.1$), where M_J = magnitude determined by the Japanese Meteorological Agency. The building responses were compared with those calculated by a base-fixed building response analysis and by a conventional soil-building interaction analysis. It was clarified that the proposed method was able to provide more appropriate building responses.

[1]Researcher, Earthquake Research Institute, Univ. of Tokyo, Yayoi, Bunkyo-ku, Tokyo 113-0032, Japan (corresponding author). E-mail: iida@eri.u-tokyo.ac.jp

[2]Professor, Dept. of Architecture, Hokkaido Univ., Sapporo 060-8628, Japan. E-mail: iiba-m@eng.hokudai.ac.jp

[3]Associate Professor, Earthquake Research Institute, Univ. of Tokyo, Tokyo, Japan. E-mail: kusunoki@eri.u-tokyo.ac.jp

[4]Professor, Dept. of Architecture, Osaka Univ., Osaka 113-0032, Japan. E-mail: miyamoto@arch.eng.osaka-u.ac.jp

[5]Professor, Research Institute for Sustainable Humanosphere, Kyoto Univ., Uji 611-0011, Japan. E-mail: hisoda@rish.kyoto-u.ac.jp

Note. This manuscript was submitted on July 5, 2016; approved on March 20, 2017; published online on June 7, 2017. Discussion period open until November 7, 2017; separate discussions must be submitted for individual papers. This paper is part of the ***International Journal of Geomechanics***, © ASCE, ISSN 1532-3641.

The present study is aimed at calculating seismic responses of a variety of buildings for some earthquake-station pairs in the reclaimed zone of Tokyo Bay by using the proposed linear method. The purpose is twofold. While the authors intend to demonstrate wide applicability of the method, the reclaimed zone with a high seismic risk and huge population requires such an evaluation. In this context, first the seismic responses of a building are calculated at two soft-soil sites for three large earthquakes to understand the variations in building responses with reference to sites and earthquakes. Second, seismic responses of low- to high-rise RC and steel buildings and wood buildings are compared at a soft-soil site for a large earthquake, evaluating the relative seismic risk of various buildings. Application of the method to steel buildings is made for the first time. The relative seismic risk is judged by several basic response values.

Although the proposed linear method is in the process of being developed, it should be useful for evaluating the relative seismic risk of various buildings if the predominant period of surface ground motions is affected little by the inelastic behavior of soils. As far as the authors know, such relative seismic risk has not been evaluated under a common condition using an advanced building response method. Throughout the present study, the authors tried not to underestimate the ground motions and the soil and building responses; perhaps this intention can be achieved because the soil and building responses will be overestimated by the linear method.

A great deal of soil-structure interaction studies have been performed. Most practical interaction studies handled RC structures in which interaction effects are regarded to be large (Guin and Banerjee 1998; Bárcena and Esteva 2007; Elgamal et al. 2008). In contrast, it should be preferable that steel and wood structures are also evaluated by a soil-structure interaction analysis. If consideration is restricted to buildings, then the interaction effects of steel and wood buildings might be small compared with those of RC buildings. However, there are two convincing reasons to encourage an interaction analysis for steel and wood buildings; they are the reasonable treatments of soil modes and ground motions, as was previously stated in this section.

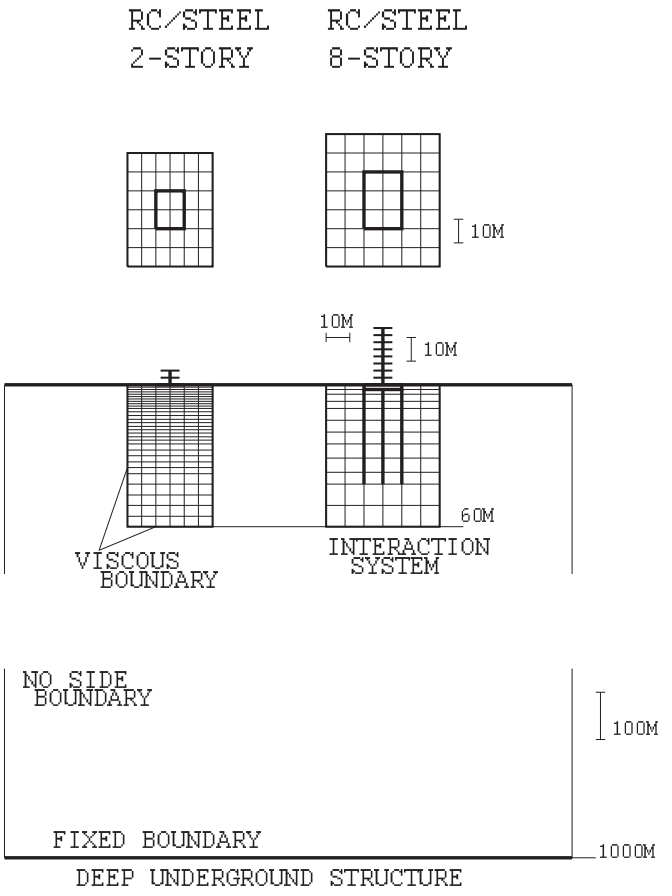

Fig. 1. Plan sections and cross sections (north-south direction) of two examples of the 3D superstructure-foundation-pile-soil systems at the Echujima station (Note: A system for the 2-story RC and steel buildings without piles and another system for the 8-story RC and steel buildings with piles are shown; one-dimensional appropriate deep underground structures, which are used to estimate input wave fields, are also displayed)

Method

This section explains the outline of the 3D linear time-domain FEM for examining the soil-building interaction based on an input seismic wave field. The method was proposed in a recent study (Iida 2013) and was improved in a subsequent study (Iida et al. 2015). The method used in the present study is the same as that used in the subsequent study (Iida et al. 2015).

Fig. 1 illustrates two examples of the 3D superstructure-foundation-pile-soil systems. The lumped-mass stick building superstructure rests on a rigid box foundation supported on piles. The superstructure is modeled as a shear spring system, and sway and rocking of the foundation are considered. The horizontal degree of freedom of each story is coupled with the rocking degree of freedom at the foundation. Each pile is modeled by beam elements, and the soil volume is modeled by 3D rectangular prism elements. To allow the relative movement (slip) of the pile with respect to the soil, joint spring elements are attached to both edges of each beam element that forms the pile. Strictly speaking, because the joint spring element is adopted, the method is not linear. In the case of a low-rise building without piles, the foundation is fixed to the soil (the left-hand system of Fig. 1). The side and bottom boundaries of the soil volume are equipped with viscous dampers.

The multilayered soil volume of the 3D interaction system is subject to horizontal ground motions. As an input wave field, vertically propagating plane S waves and horizontally propagating plane surface waves are imposed on the soil volume of the 3D system. An S-wave field and a surface-wave field are separately estimated in the soil volume by applying elastic wave theory to an appropriate deep underground structure, after surface ground motions are separated into S waves and surface waves. The whole-wave field used as input is the summation of the two wave fields.

Once again, an input wave field is used to treat surface waves trapped in a deep underground structure adequately. The significance of an input wave field will be shown in the next section. The most relevant examples that demonstrate the obvious effects of soil responses due to an input wave field are given in Iida et al. (2015, Figures 6–8), which investigated seismic responses of the 8-story RC building and the 2-story wood building used in the present study.

Soil Responses

In the present study, because a variety of buildings are used, the two horizontal components of ground motions are treated in a wide period range between 0.1 and 5.0 s. Although long-period ground motions with periods of more than several seconds and a very deep underground structure corresponding to the long-period ground

motions are not negligible for building responses in the soft Kanto sedimentary basin on which the reclaimed zone of Tokyo Bay is situated (Koketsu and Higashi 1992; Hisada et al. 1993), the long-period ground motions are beyond the scope of the present study. Presumably, the long-period ground motions should cause large displacements of the upper stories of a very tall building.

Because the features of the two horizontal components did not differ from each other significantly in the reclaimed zone of Tokyo Bay in a ground motion study (Iida et al. 2005), only the north-south components are displayed. Prior to the present study, soil responses based on an input seismic wave field were successfully calculated for three large earthquakes at two (Echujima and Toyo) borehole stations located in the reclaimed zone in a soil response study (Iida 2006). In this section, important results of the soil response study are reviewed. For the details, please see the previously mentioned studies.

In the soil response study, S-wave and surface-wave accelerograms were synthesized on the ground surface at two stations for three large earthquakes. The surface fault geometries of the three large earthquakes are projected in Fig. 2. First, the 1855 Ansei-Edo earthquake ($M_J = 7.4$) was an inland deep event, and the Tokyo metropolitan area suffered heavy damage. Second, the 1923 Kanto earthquake, which was a well-known offshore shallow event, caused the heaviest damage historically to the metropolitan area. Wald and Somerville (1995) interpreted that northern parts of the fault zone, which were very close to the metropolitan area, did not break very much during the large event. Their interpretation implies that the metropolitan area is likely to suffer higher intensity ground motions in the long run. Third, and for this reason, a hypothetical Saitama earthquake ($M_J = 7.7$) was assumed as the most devastating inland event.

The whole-wave acceleration time series synthesized on the ground surface at the Echujima station for the three large earthquakes are displayed in Fig. 3. The time series are the sums of the synthesized S-wave and surface-wave ones. The maximum acceleration of the Ansei-Edo earthquake is at best 5 m/s^2. The accelerogram of the Kanto earthquake has a main-motion duration of about 30 s, and the peak amplitude reaches 10 m/s^2. As for the Saitama earthquake, the large-amplitude (about 30 m/s^2) wave trains with a short duration of about 15 s are quite impressive. These very large amplitudes are probably due to linear soil modeling. The Fourier spectra indicate that the predominant period of the ground motions is about 1.0 s (1.0 Hz) and coincides well with the theoretical predominant period of the ground. Also, the ground motions contain a great deal of short-period components between 0.2 and 0.5s. The short-period components will turn out to be very important for building responses.

In contrast, the amplitudes of the surface accelerograms were almost two times larger than those at the Toyo station. The predominant periods of the surface accelerograms were much the same at the two stations. In a ground motion study (Iida et al. 2005), the remarkable difference in the amplitudes between the two stations was interpreted to be due to surface waves. In the soft surface layers at the two stations, surface waves had a vertical amplitude increase larger than S waves. Accordingly, the difference in the amplitudes of the surface accelerograms was caused by the difference in the ratio of surface waves included in the surface accelerograms. In other words, the ground motions at the Echujima station contained a considerable amount of surface waves, whereas those at the Toyo station were mostly S waves. The ground motions are very sensitive to local site effects. Therefore, the amplitudes of the ground motions at the Echujima and the Toyo stations are regarded to roughly correspond to the upper and lower limits in the reclaimed zone of Tokyo Bay, respectively.

In the soil response study, in a 3D soil model, an S-wave and surface-wave fields were estimated from the S-wave and surface-wave accelerograms synthesized at the surface and an appropriate deep underground structure (Fig. 1). Table 1 shows the deep underground structural model used at the Echujima station, which was obtained in the ground motion study (Iida et al. 2005). The structural

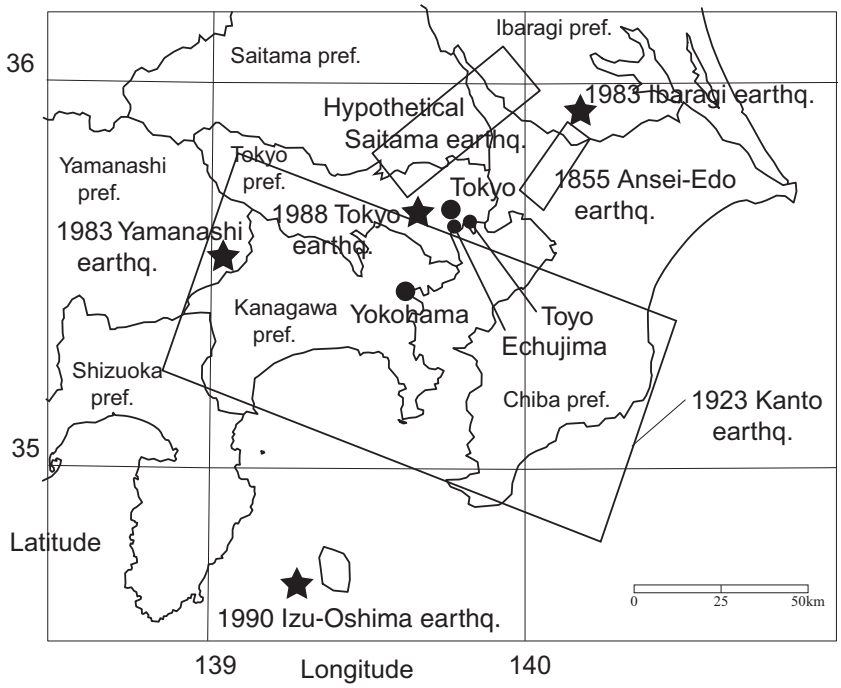

Fig. 2. Location map of the Kanto region of Japan; the surface fault geometries of the three large earthquakes are projected; the accelerograms recorded during the medium-sized events were used as Green's functions to synthesize the accelerograms for the three large events (Note: The Echujima and the Toyo borehole stations are shown by small solid circles, and the epicenters of four medium-sized earthquakes are marked with solid stars) (reprinted from Iida 2006, © ASCE)

model is characterized by a soft silty surface deposit as well as the soft Kanto sedimentary basin. Remarkably, the basin with a thickness of about 1.5 km is extremely soft. Thus, the entire model of Table 1 excites and traps short-period surface waves greatly. A wave field used as input was obtained by summing the two wave fields.

Finally, a soil response analysis was conducted using the 3D soil model. The spatial discretization of soil-element sizes is made, taking into account such factors as the vibration period of the building, the minimum period required in the interaction analysis, and the pile behavior near the ground surface. Because the soft surface layers have very low S-wave velocities, the vertical heights of soil elements get very small in the soft layers (Fig. 1).

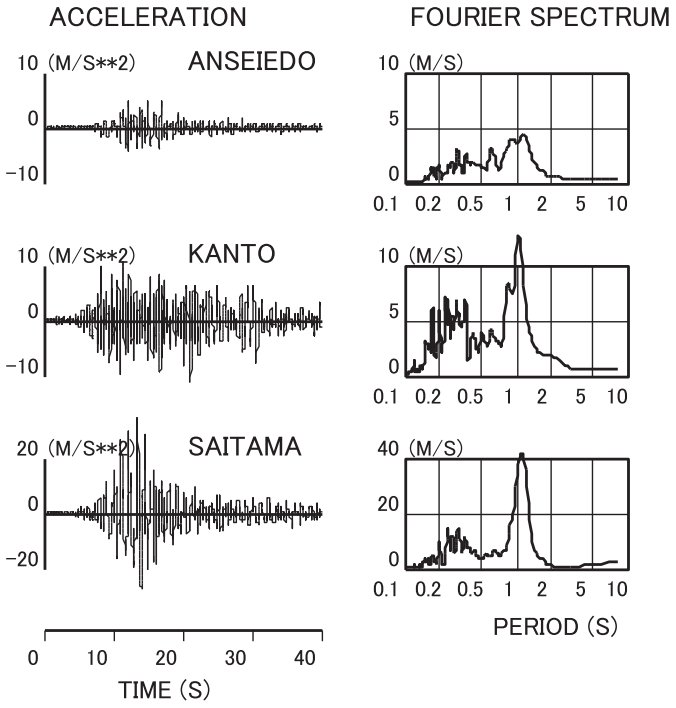

Fig. 3. Surface accelerograms synthesized at the Echujima station for the three large earthquakes

Table 1. Deep Underground Structural Model Used at the Echujima Station

Depth (m)	P-wave velocity (m/s)	S-wave velocity (m/s)	Density (t/m^3)	Damping factor
0–4	620	110	1.70	0.045
4–10	940	110	1.70	0.045
10–16	1,330	130	1.60	0.038
16–26	1,330	130	1.70	0.038
26–34	1,330	230	1.70	0.022
34–38	930	230	1.70	0.022
38–53	1,750	440	2.00	0.011
53–70	1,750	440	1.85	0.011
70–75	1,750	300	1.85	0.017
75–83	1,750	460	1.85	0.011
83–100	1,750	460	1.90	0.011
100–210	1,830	500	1.90	0.010
210–1,000	1,830	880	1.90	0.006
≥1,000	1,830	880	1.90	0.006

It was confirmed that an input wave field was well retrieved as FE-simulated soil responses based on the input wave field. In contrast, a lack of fit was revealed between an input wave field and FE-simulated soil responses based on an input base motion. The lack of fit was caused because the large vertical increase in the amplitudes of surface waves in the soft surface layers could not be expressed on the basis of an input base motion. In addition, the soil response study performed a nonlinear and liquefaction soil response analyses, which indicated that the predominant period of surface ground motions was affected little by the inelastic behavior of soils. This result is very significant for the present study.

Model Buildings

This section describes RC, steel, and wood model buildings used in the present study. On the basis of the Japanese building codes (Building Center of Japan 2013), five RC buildings, five steel buildings, and two wood buildings were modeled. The five RC or steel buildings are 2-, 5-, 8-, 15-, and 30-story buildings, and the two wood buildings are 2- and 3-story buildings. In principle, standard model buildings with small foundation dimensions are used to reduce computational burden. Low-rise (1- and 2-story) RC and steel buildings and all wood buildings of no more than three stories do not need piles.

First, RC buildings were modeled. The base shear coefficient C_B was supposed to be 0.30 for all buildings. Triangular distributions were assumed for the stiffness and the shear strength, and the yield stiffness was used for the stiffness. The parameter values of the top five stories were set to be equal to those of the fifth story from the top. In the cases of the 2- and 5-story buildings, the parameter values of all stories were set to be the same as those of the first story. Also, it was assumed that the mass of the foundation was equal to 10% of the mass of the superstructure, and that the embedment of the foundation was equal to 6% of the height of the superstructure. The parameters used for the superstructures and the foundations thus evaluated are summarized in Table 2. In the cases of the 2- and 5-story buildings, because of computational difficulty, the thin (less than 0.9-m) embedment of the foundation was not considered, and a foundation model without the embedment was adopted.

Because the pile tip needs to reach enough stiff-soil layers to support the building, a pile length of about 40 m is required at the two soft-soil sites. The pile radius was determined such that the piles support the total mass of the superstructure and the foundation. The pure and the maximum yield bending moments are obtained by an axial force-bending moment yield curve of the pile. The parameters used for the piles thus evaluated are listed in Table 3.

Second, regarding steel model buildings, the structural parameters were evaluated in much the same way as the RC buildings, by using a C_B of 0.25 for all buildings. The mass of the foundation was assumed to be equal to 20% of the mass of the superstructure, and the embedment of the foundation was assumed to be equal to 6% of the height of the superstructure. Table 4 summarizes the parameters used for the superstructures and the foundations. The parameters used for the piles were also evaluated following a same procedure similar to the RC buildings, and these are listed in Table 5.

Third, the layout of the plan section of a wood building is arbitrary, so the structural parameters have large variations, compared with a RC building or a steel building. Also, the foundation of a wood building is designed independently of the light superstructure because the mass of the foundation is heavier than the mass of the superstructure. Hence, the wood model buildings used here should be regarded as typical examples. The parameters used for the superstructures and the foundations are summarized in Table 6. They are designed in

Table 2. Parameters Used for the Superstructures and the Foundations of the Five RC Buildings

Building (number of stories)	Superstructure					Foundation		
	Height of each story (m)	Mass of each story (t)	Stiffness of each story (10^6 kN/m)[a]	Yield shear strength of each story (kN)[a]	Fundamental period [s (Hz)]	Mass (t)	Embedment (m)	Dimensions (m^2)
2	3	255	0.93	1,497	0.17 (5.88)	51	0	192
5	3	382	1.06	5,616	0.42 (2.38)	191	0	288
8	3	509	1.192 (4–8)	4,991 (4–8)				
			1.231 (3)	6,988 (3)	0.68 (1.47)	402	2	384
			1.651 (1)	11,976 (1)				
15	3	509	0.966 (11–15)	2,668 (11–15)				
			1.006 (10)	3,735 (10)	1.27 (0.79)	764	2	384
			1.739 (1)	21,335 (1)				
30	3	764	0.320 (26–30)	820 (26–30)	2.55 (0.39)	2,496	6	576
			0.358 (25)	1,148 (25)				
			1.613 (1)	25,421 (1)				

[a]The numerical values in parentheses are story numbers.

Table 3. Parameters Used for the Concrete-Filled Steel Piles of the Four RC Buildings

Building (number of stories)	Number	Length (m)	Radius (m)	Elastic modulus (kN/m^2)	Density (t/m^3)	Pure yield bending moment[a] (kN · m)	Maximum yield bending moment (kN · m)
5	12	42	0.5	1.47×10^7	2.4	1,600	2,600
8	12	40	0.5	1.47×10^7	2.4	1,600	2,600
15	12	40	0.7	1.47×10^7	2.4	4,390	7,130
30	20	36	1	1.47×10^7	2.4	12,800	20,800

[a]The pure yield bending moment indicates the yield bending moment without the axial force.

Table 4. Parameters Used for the Superstructures and the Foundations of the Five Steel Buildings

Building (number of stories)	Superstructure					Foundation		
	Height of each story (m)	Mass of each story (t)	Stiffness of each story (10^6 kN/m)[a]	Yield shear strength of each story (kN)[a]	Fundamental period [s (Hz)]	Mass (t)	Embedment (m)	Dimensions (m^2)
2	3.0	157	0.509	768	0.18 (5.56)	63	0.0	192
5	3.0	235	0.580	2,880	0.45 (2.22)	235	0.0	288
8	3.0	313	0.652 (4–8)	2,539 (4–8)	0.72 (1.39)	502	2.0	384
			0.674 (3)	3,555 (3)				
			0.904 (1)	6,095 (1)				
15	3.0	313	0.528 (11–15)	1,024 (11–15)	1.35 (0.74)	940	2.0	384
			0.551 (10)	1,434 (10)				
			0.951 (1)	8,191 (1)				
30	3.0	470	0.350 (26–30)	396 (26–30)	2.70 (0.37)	2,821	6.0	576
			0.392 (25)	555 (25)				
			1.765 (1)	12,289 (1)				

[a]The numerical values in parentheses are story numbers.

Table 5. Parameters Used for the Concrete-Filled Steel Piles of the Four Steel Buildings

Building (number of stories)	Number	Length (m)	Radius (m)	Elastic modulus (kN/m^2)	Density (t/m^3)	Pure yield bending moment[a] (kN · m)	Maximum yield bending moment (kN · m)
5	12	42	0.5	1.47×10^7	2.4	1,600	2,600
8	12	40	0.5	1.47×10^7	2.4	1,600	2,600
15	12	40	0.55	1.47×10^7	2.4	2,130	3,460
30	20	36	0.8	1.47×10^7	2.4	6,550	10,650

[a]The pure yield bending moment indicates the yield bending moment without the axial force.

accordance with the minimum requirement of Japanese Building Standard Law. Because of computational difficulty, the thin (0.54-m) embedment of the foundation was not considered, and a foundation model without the embedment was adopted.

In the present study, since linear building responses are calculated, a common damping factor was adopted for the RC, steel, and wood buildings. In a companion study (Iida et al. 2015), in which building responses due to an input wave field were calculated in the reclaimed zone of Tokyo Bay, a damping factor h of 0.05 was evaluated on the basis of the recordings of a real building, and it was used for two model buildings. In the present study, a common damping factor h of 0.05 was used for all model buildings. The horizontal stiffness and the vertical stiffness of the joint spring element that connects a node for the pile and another node for the soil are also the same values as those used in the companion study, and they worked well throughout the present study.

Responses of a Midrise RC Building at Two Sites for Three Earthquakes

In this section, seismic responses of a building are calculated at the two soft-soil sites for the three large earthquakes to understand the variations in building responses with reference to sites and earthquakes. Seismic responses of the 8-story RC building were calculated at the Echujima and the Toyo station for the 1855 Ansei-Edo, the 1923 Kanto, and a hypothetical Saitama earthquake. In the present study, all building responses were computed for 40 s with a time interval of 0.01 s. The 8-story RC building was selected because the fundamental period (0.68 s; 1.47 Hz) of the building is somewhat shorter than the predominant periods (about 1.0 s; 1.0 Hz) of the grounds at the two stations. Because the vibration period of the building was extended due to interaction effects, the building resonated severely with ground motions. The top-story accelerogram is exhibited as the second trace of Fig. 4. The maximum response values of the superstructure of the building are compared among four earthquake-station pairs in Table 7.

Because of both the linear soil behavior and the linear building behavior, the superstructural responses are very large in all the pairs, suggesting heavy damage. The pile responses were also very large in all the pairs, suggesting heavy damage. Only the pile response for a single pair of the Echujima station and the Kanto earthquake is given in Table 8. These results seem to imply that the superstructure suffers more damage than the pile, considering that the bending moment at the pile head can be somewhat overestimated because of the rigid connection between the pile and the

Table 6. Parameters Used for the Superstructures and the Foundations of the Two Wood Buildings

	Superstructure					Foundation		
Building (number of stories)	Height of each story (m)	Mass of each story (t)	Stiffness of each story (kN/m)[a]	Yield shear strength of each story (kN)[a]	Fundamental period [s (Hz)]	Mass (t)	Embedment (m)	Dimensions (m^2)
2	2.7	5.60 (2)	706 (2)	16.05 (2)	0.74 (1.35)	36.9	0	60
		10.20 (1)	1,663 (1)	37.84 (1)				
3	2.7	8.82 (3)	1,209 (3)	27.52 (3)	0.95 (1.05)	36.9	0	60
		10.20 (1–2)	1,966 (2)	44.72 (2)				
			2,520 (1)	57.33 (1)				

[a]The numerical values in parentheses are story numbers.

Table 7. Maximum Response Values of the Superstructure of the 8-Story RC Building at the Two Stations for the Three Large Earthquakes

Earthquake	Station	Acceleration (m/s^2)	Displacement (m)	Drift (m)	Ratio (%)
Kanto	Echujima	38.42	0.402	0.072	795
Kanto	Toyo	23.12	0.200	0.036	404
Ansei-Edo	Echujima	21.31	0.237	0.042	474
Saitama	Echujima	105.10	1.230	0.225	2,611

Note: Acceleration indicates the top-story absolute acceleration with rocking, and the displacement indicates the top-story relative displacement with rocking with respect to the foundation. Drift denotes the maximum interstory drift through all stories, and ratio denotes the shear force/yield strength ratio of the first story.

Table 8. Maximum Response Values at the Heads of Corner Piles of the Eight Buildings with Piles at the Echujima Station for the 1923 Kanto Earthquake

Building	Shear force (kN)	Axial force (kN)	Bending moment (kN · m)	Maximum yield bending moment (kN · m)	Ratio (%)
RC5	3,303	10,584	8,085	2,600	311
S5	2,244	6,419	5,655	2,600	218
RC8	7,634	31,850	9,731	2,600	374
S8	4,283	19,698	5,625	2,600	216
RC15	7,291	34,104	9,506	7,130	133
S15	4,312	20,874	5,674	3,460	164
RC30	7,340	22,246	1,7346	2,0800	83
S30	6,850	23,618	1,1564	1,0650	109

Note: Ratio denotes the ratio of the bending moment to the maximum yield value.

foundation. Pile responses will be discussed in the next section. Regarding the 8-story RC building and the 2-story wood building, which will be used in the next section, the linear responses for the Kanto earthquake were already calculated and were compared with those calculated by two standard analyses in a recent study (Iida et al. 2015). Thus, the superiority of the reasonable responses was already confirmed.

The maximum response values of the superstructure at the two stations for the Kanto earthquake (Table 7) show that the responses at the Echujima station are almost two times larger than those at the Toyo station. This result is quite consistent with the result mentioned in a previous section, which showed that the amplitudes of surface ground motions at the Echujima station were almost two times larger than those at the Toyo station. Furthermore, on the basis of an interpretation addressed in the same section, the superstructural responses obtained at the Echujima and the Toyo stations roughly correspond to the upper and lower limits in the reclaimed zone of Tokyo Bay, respectively.

As for the maximum response values of the superstructure at the Echujima station for the three large earthquakes (Table 7), first, the responses for the Ansei-Edo earthquake are nearly half of those for the Kanto earthquake. As is inferred from the surface ground motions in Fig. 3, ground motions during the Kanto earthquake are more destructive than those during the Ansei-Edo earthquake in all aspects, such as the maximum amplitude and the duration of main motions. Second, the superstructural responses for a hypothetical Saitama earthquake are about three times larger than those for the Kanto earthquake. This result appears to warn of a devastating inland event in the Tokyo metropolitan area.

Responses of Various Buildings

In this section, seismic responses of the RC, steel, and wood buildings are compared under a common condition with the goal of evaluating the relative seismic risk of various buildings. Seismic responses of the five RC buildings, the five steel buildings, and the two wood buildings are calculated at the Echujima station for the 1923 Kanto earthquake. The maximum response values of the superstructures of the 12 buildings are summarized in Table 9.

First, it should be noted that the interstory drifts of the two wood buildings reach a few tens of centimeters. In spite of the heights of the two buildings lower than 10 m, the top-story displacements are extraordinarily large. The large deformations indicate an inherent feature of the wood buildings. The two buildings resonated severely with ground motions (Fig. 4) because the fundamental periods (0.74 and 0.95 s; 1.35 and 1.05 Hz) of the buildings are close to the predominant period (about 1.0 s; 1.0 Hz) of the ground. Second, the superstructural responses of a RC building and a steel building with the same story number have a similar pattern because the fundamental periods of the RC and the steel building are close to each other.

Third, the superstructural responses of RC and steel buildings with different story numbers are characterized by larger responses of midrise buildings than low-rise and high-rise buildings. The relative responses are intuitionally understandable on the basis of the fundamental periods of the buildings. Remarkably, the responses of the 5-story RC and steel buildings, which have much shorter fundamental periods (0.42 and 0.45 s; 2.38 and 2.22 Hz) than the predominant period of the ground, are very large. The large responses are induced by a great deal of short-period components around the fundamental periods of the buildings (Fig. 3), which is pointed out in a previous section. Thus, midrise buildings are likely to sustain severe damage. Fourth, the interstory drifts of the low-rise RC and steel buildings are quite small, whereas the shear forces of the high-rise RC and steel buildings are not very large. Therefore, low-rise and high-rise buildings are regarded as basically safe.

For confirmation of the response patterns, Fig. 5 exhibits the vertical distributions of the maximum interstory drift and the maximum shear force of four representative buildings. The four buildings are

Table 9. Maximum Response Values of the Superstructures of the 12 Buildings at the Echujima Station for the 1923 Kanto Earthquake

Building	Acceleration (m/s^2)	Displacement (m)	Drift (m)	Ratio (%)
RC2	18.79	0.017	0.011	683
S2	20.19	0.020	0.013	858
RC5	31.57	0.125	0.036	688
S5	35.62	0.157	0.045	899
RC8	38.42	0.402	0.072	795
S8	37.09	0.447	0.081	968
RC15	21.76	0.439	0.039	238
S15	21.15	0.493	0.044	380
RC30	11.78	0.516	0.077	149
S30	18.20	0.544	0.088	430
W2	32.23	0.482	0.250	1,031
W3	46.36	1.010	0.354	1,427

Note: Explanations are listed in Table 7.

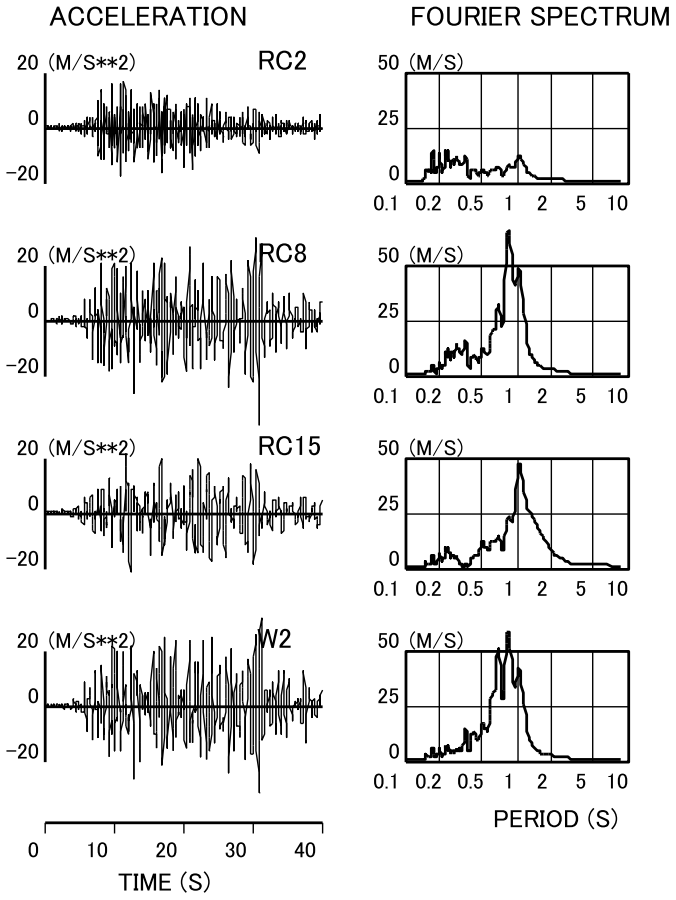

Fig. 4. Top-story absolute accelerograms with rocking of the four buildings at the Echujima station for the 1923 Kanto earthquake (the four buildings are the 2-, 8-, and 15-story RC buildings and the 2-story wood building)

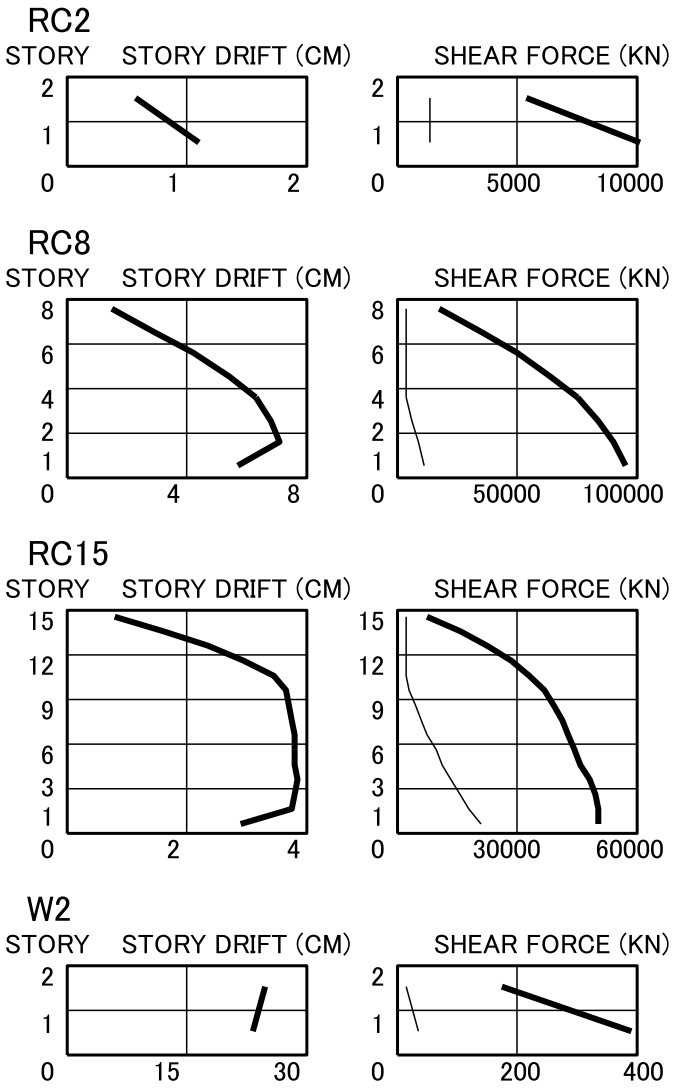

Fig. 5. Vertical distributions of the maximum interstory drift and the maximum shear force of the four buildings at the Echujima station for the 1923 Kanto earthquake (thick lines) (Note: The straight thin lines indicate the yield strength; the four buildings are the 2-, 8-, and 15-story RC buildings and the 2-story wood building)

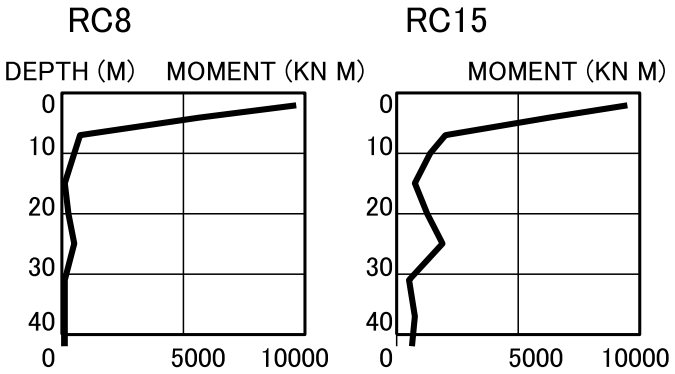

Fig. 6. Vertical distributions of the maximum bending moment of corner piles of the 8- and 15-story RC buildings at the Echujima station for the 1923 Kanto earthquake

the 2-, 8-, and 15-story RC buildings and the 2-story wood building, which are representative of low-, mid-, and high-rise RC and steel buildings and wood buildings, respectively. In all four buildings, the shear force of each story largely exceeded the yield strength. In contrast, large differences in the building responses are observed regarding the interstory drift. The interstory drifts appear to suggest the relative risk of the buildings.

These results can be interpreted properly on the basis of the fundamental periods of the buildings and the predominant period of the ground. Fig. 4 displays the top-story acceleration time histories of the four buildings. First, the fundamental period (0.17s; 5.88 Hz) of the 2-story RC building, which corresponds to a natural period of high order of the interaction system, is far away from the predominant period of the ground, which corresponds to the first-order natural period of the interaction system. Consequently, the building shakes with the long predominant period of the ground as well as the short fundamental period of the building. The top-story accelerations remain modest relative to the surface accelerations.

Next, as was already shown in the last section, the 8-story RC building resonates severely with ground motions. So, the top-story accelerations get very large. As for the 15-story RC building, although the first-order vibration mode of the interaction system is a building mode, there was a small amount of ground motions with periods close to or longer than the fundamental period (1.27 s; 0.79 Hz) of the building (Fig. 3). As a result, the building vibrates mainly with a soil mode that corresponds to the second-order vibration mode of the interaction system, not with a building mode. Hence, the top-story accelerations do not get very large compared with those of the 8-story building.

Finally, the top-story acceleration time history of the 2-story wood building is similar to that of the 8-story RC building. Originally, the fundamental period (0.74 s; 1.35 Hz) of the wood building is slightly longer than that of the RC building. During the strong shaking, while the vibration period of the RC building was extended due to interaction effects, the vibration period of the wood building remained unchanged. Accordingly, the vibration periods of the two buildings got almost the same. In contrast, the wood building is much more flexible than the RC building, so the deformations of the two buildings are quite different (Table 9).

Table 8 lists the maximum response values at the heads of the corner piles of the midrise and high-rise RC and steel buildings. The piles of the 5- and 8-story buildings are subject to very large bending moments beyond the moment capacities, implying heavy damage. Generally, the bending moment of a pile is produced by both vibration of the superstructure and vibration of the soil. In a companion study (Iida et al. 2015) in which the contributions of the two sorts of vibrations to the bending moment at the head of a corner pile of the identical 8-story RC building were measured at the Echujima station for the Kanto earthquake, the contribution of vibration of the superstructure occupied about three-fourths of the bending moment. This result suggests that the pile response depends basically on vibration of the superstructure at the Echujima station. In contrast, the pile responses of the 30-story buildings are moderate and do not seem to cause pile damage. The pile responses of the 15-story buildings indicate an intermediate character of these two results.

Also, Fig. 6 presents the vertical distributions of the maximum bending moment of the same corner piles of the 8- and 15-story RC buildings. The largest bending moments were induced at the head portions in both buildings. Considering the maximum yield bending moment (Table 8), pile damage of the 8-story building is anticipated to occur much more. Thus, the pile responses are quite consistent

with the previously mentioned superstructural responses. On the basis of the response values summarized in Tables 8 and 9, superstructural damage is likely to occur rather than pile damage.

Discussion

The unique value of the present study is the comprehensive evaluation of seismic responses of the three types of buildings based on an input wave field, which enabled the authors to reproduce reasonable soil responses. Although the current interaction model might have some drawbacks, it provided probable basic responses in the present study. A series of building simulations showed that RC and steel buildings had considerable similarities in dynamic behavior (Tables 8 and 9). In contrast, the flexible dynamic behavior of wood buildings was remarkable (Figs. 4 and 5).

The measurement of seismic risk, the absolute acceleration and the relative displacement, both of which include rocking, did not indicate distinct characteristics of building responses (Table 9). The interstory drift, which is independent of rocking, and the shear force were good measurements to express seismic risk. In particular, the interstory drift appeared to be the best measurement for the superstructure. As for the pile foundation, the bending moment at the pile head is considered to be the best measurement (Table 8). These response values disclosed that the superstructure sustained more damage than the pile.

In an earlier section of the article it was shown that low- and high-rise RC and steel buildings were basically safe at the Echujima station. Also, in a different section, the building responses obtained at the Echujima station were interpreted to be roughly the maximum in the reclaimed zone of Tokyo Bay. Taking these opinions and the linear soil and building behavior into account, it can be concluded that low- and high-rise RC and steel buildings are considerably safe in the reclaimed zone of Tokyo Bay.

Presumably, the current linear interaction model has two drawbacks. First, if the predominant period of surface ground motions is changed largely by the inelastic behavior of soils, the building responses obtained might be invalid. Second, the simplified superstructural model used is unable to consider torsional vibration or detailed behavior and damage of the building including the joint sections. However, the authors might emphasize that the comprehensive evaluation made in the present study should hold in spite of the two drawbacks.

In the present study, a linear soil-building interaction analysis was performed. Because linear responses are not practical, a nonlinear (Bárcena and Esteva 2007; Zhang et al. 2008) or liquefaction (Maheshwari and Sarkar 2011; Shafieezadeh et al. 2013) soil-structure interaction analysis is required hereafter. In the current method, it is easy to treat nonlinearity of the superstructure and the piles. Also, it is feasible to treat soils acting in a nonlinear or liquefaction fashion, and such behavior of soils might change a seismic wave field. In a soil response study based on an input seismic wave field (Iida 2006), the nonlinear and liquefaction behavior of soils was already taken into account.

Conclusions

Seismic responses of various buildings were calculated by a 3D linear method for examining the soil-building interaction based on an input seismic wave field in the reclaimed zone of Tokyo Bay in which ground motions include a considerable amount of surface waves. First, seismic responses of a building were calculated at two soft-soil sites for three large earthquakes to understand the variations in building responses with reference to sites and earthquakes. Second, seismic responses of low- to high-rise RC and steel buildings and wood buildings were compared at a soft-soil site for a large earthquake, evaluating the relative seismic risk of various buildings.

The main conclusions of the two simulations include the following: (1) the first simulation successfully indicated the degree of differences in building responses due to the site and the earthquake; (2) in the second simulation, it was clarified that midrise RC and steel buildings shook more severely than low- and high-rise RC and steel buildings; (3) it was disclosed that the superstructure sustained more damage than the pile; and (4) it was also clarified that flexible wood buildings suffered extremely large interstory drifts, indicating the largest seismic risk.

Acknowledgments

Most of the accelerograms were provided as a data set of Strong Motion Array Observation No. 2 by the Association for Earthquake Disaster Prevention of Japan (1995). Parts of the accelerograms recorded at the Echujima station were supplied by the Shimizu Corporation of Japan. Dr. Tetsuya Ishihara of the Technical Research and Development Institute, JDC Corporation of Japan, gave helpful advice on the soil-building interaction system. Dr. Masaomi Teshigawara of Nagoya University of Japan gave instructive advice on steel buildings. Two anonymous reviewers greatly improved the manuscript.

References

Bárcena, A., and Esteva, L. (2007). "Influence of dynamic soil-structure interaction on the nonlinear response and seismic reliability of multistorey systems." *Earthquake Eng. Struct. Dyn.*, 36(3), 327–346.

Bielak, J., and Christiano, P. (1984). "On the effective seismic input for non-linear soil-structure interaction systems." *Earthquake Eng. Struct. Dyn.*, 12(1), 107–119.

Building Center of Japan. (2013). *The building standard law of japan (enforcement order of building standard law)*, Chapter 3, Section 8, Tokyo.

Elgamal, A., Yan, L., Yang, Z., and Conte, J. (2008). "Three-dimensional seismic response of bridge foundation-ground system." *J. Struct. Eng.*, 10.1061/(ASCE)0733-9445(2008)134:7(1165), 1165–1176.

Flores-Berrones, R., and Whitman, R. V. (1982). "Seismic responses of end-bearing piles." *J. Geotech. Engrg. Div.*, 108(4), 555–569.

Guin, J., and Banerjee, P. (1998). "Coupled soil-pile-structure interaction analysis under seismic excitation." *J. Struct. Eng.*, 10.1061/(ASCE)0733-9445(1998)124:4(434), 434–444.

Hisada, Y., Aki, K., and Teng, T. (1993). "3-D simulations of surface wave propagation in the Kanto sedimentary basin, Japan, Part 2: Application of the surface wave BEM." *Bull. Seismol. Soc. Am.*, 83(6), 1700–1720.

Housner, G. W. (1957). "Interaction of building and ground during an earthquake." *Bull. Seismol. Soc. Am.*, 47(3), 179–186.

Iida, M. (2006). "Three-dimensional linear and simplified nonlinear soil response methods based on an input wave field." *Int. J. Geomech.*, 10.1061/(ASCE)1532-3641(2006)6:5(342), 342–355.

Iida, M. (2013). "Three-dimensional finite-element method for soil-building interaction based on an input wave field." *Int. J. Geomech.*, 10.1061/(ASCE)GM.1943-5622.0000232, 430–440.

Iida, M., Iiba, M., Kusunoki, K., Miyamoto, Y., and Isoda, H. (2015). "Seismic responses of two RC buildings and one wood building based on an input wave field." *Int. J. Geomech.*, 10.1061/(ASCE)GM.1943-5622.0000444, 04014093.

Iida, M., Yamanaka, H., and Yamada, N. (2005). "Wavefield estimated by borehole recordings in the reclaimed zone of Tokyo Bay." *Bull. Seismol. Soc. Am.*, 95(3), 1101–1119.

Koketsu, K., and Higashi, S. (1992). "Three-dimensional topography of the sediment/basement interface in the Tokyo metropolitan area, central Japan." *Bull. Seismol. Soc. Am.*, 82(6), 2328–2349.

Maheshwari, B., and Sarkar, R. (2011). "Seismic behavior of soil-pile-structure interaction in liquefiable soils: parametric study." *Int. J. Geomech.*, 10.1061/(ASCE)GM.1943-5622.0000087, 335–347.

Shafieezadeh, A., DesRoches, R., Rix, G., and Werner, S. (2013). "Three-dimensional wharf response to far-field and impulsive near-field ground motions in liquefiable soils." *J. Struct. Eng.*, 10.1061/(ASCE)ST.1943-541X.0000642, 1395–1407.

Wald, D. J., and Somerville, P. G. (1995). "Variable-slip rupture model of the great 1923 Kanto, Japan, earthquake: Geodetic and body-waveform analysis." *Bull. Seismol. Soc. Am.*, 85(1), 159–177.

Zhang, Y., Conte, J. P., Yang, Z., Elgamal, A., Bielak, J., and Acero, G. (2008). "Two-dimensional nonlinear earthquake response analysis of a bridge-foundation-ground system." *Earthquake Spectra*, 24(2), 343–386.